DMD Fast Forward. Published on September 8, 2011 as doi:10.1124/dmd.111.040782




# Title Page

Systemic- and direct nose-to-brain transport in the rat; a pharmacokinetic model for remoxipride after intravenous and intranasal administration

Jasper Stevens, Bart A. Ploeger, Piet H. van der Graaf, Meindert Danhof, Elizabeth C.M. de Lange

Primary laboratory of origin;

Division of Pharmacology, Leiden-Amsterdam Center for Drug Research, Leiden University, Leiden, the Netherlands (J.S., M.D., E.C.M.d L.)

LAP&P Consultants B.V., Leiden, The Netherlands (B.A.P.)

Pfizer, Pharmacometrics/Global Clinical Pharmacology, Sandwich, Kent, England (P.H. vd G.)



 

# Running title page

Running head; systemic- and direct nose-to-brain transport

Corresponding author:

Elizabeth C.M. de Lange, PhD

LACDR/Pharmacology, Leiden University

Gorlaeus Laboratories

Einsteinweg 55, 2333 CC Leiden. NL

Tel +31 (0)71 527 6330 / +31 (0)71 527 6211

Fax: +31 (0)71 527 6292

Email: l.lange@lacdr.leidenuniv.nl

# text pages: 16

# tables; 2

# figures; 4

# references; 33

# words in Abstract; 229

# words in Introduction; 670

# words in Discussion; 1298

DMD Fast Forward. Published on September 8, 2011 as DOI: 10.1124/dmd.111.040782
This article has not been copyedited and formatted. The final version may differ from this version.



list of nonstandard abbreviations in document;

AUC, area under the curve; BBB, blood-brain barrier; CL, clearance; $C_{max}$, maximal concentration; CNS, central nervous system; CSF, cerebral spinal fluid; CV, coefficient of variation; ECF, extracellular fluid; F, bioavailability; IIV, inter-individual variability; IN, intranasal; IV, intravenous; k, (elimination) rate constant; ka, absorption rate constant; OFV, objective function value; PD, pharmacodynamic; PK, pharmacokinetic; Q, intercompartmental clearance; V, volume of distribution; VPC, visual predictive check.

## Abstract

Intranasal (IN) administration could be an attractive mode of delivery for drugs targeting the central nervous system (CNS) potentially providing a high bioavailability due to avoidance of a hepatic first-pass effect and rapid onset of action. However, controversy remains whether a direct transport route from the nasal cavity into the brain exists. Pharmacokinetic modeling is proposed to identify the existence of direct nose-to-brain transport in a quantitative manner. The selective dopamine-D2 receptor antagonist remoxipride was administered at different dosages, in freely moving rats, by the IN and intravenous (IV) route. Plasma- and brain extracellular fluid (ECF) concentration-time profiles were obtained, and simultaneously analyzed using non-linear mixed effects modeling. Brain ECF/plasma AUC ratios were 0.28 and 0.19 after IN and IV administration, respectively. A multi compartment pharmacokinetic model with two absorption compartments (nose-to-systemic and nose-to-brain) was found to best describe the observed pharmacokinetic data. Absorption was described in terms of bioavailability and rate. Total bioavailability following IN administration was 89%, of which 75% was attributed to direct nose-to brain transport. Direct nose-to-brain absorption rate was slow, explaining prolonged brain ECF exposure after IN compared to IV administration. These studies explicitly provide separation and quantitation of systemic- and direct nose-to-brain transport after IN administration of remoxipride in the rat. Describing remoxipride pharmacokinetics at the target site (brain ECF) in a semi-physiology based manner would allow for better prediction of pharmacodynamic effects.

# Introduction

Many diseases, including Parkinson's disease, schizophrenia and depression are related to dysfunctions of the dopaminergic system in the central nervous system (CNS). The effects of therapeutic agents following oral administration are often limited due to active first-pass clearance by the liver and restricted blood-brain barrier (BBB) transport. In theory, direct injections into the brain, by intracerebroventricular or intraparenchymal injections, are an alternative to the oral route. However, these methods are invasive and risky and therefore not suitable for application in clinical practice. Moreover, local injection does not always result in sufficient CNS target site distribution, as brain diffusion may be slow relative to elimination processes (De Lange, et al., 1995; Dhuria, et al., 2009).

Intranasal (IN) administration could be an attractive alternative mode of delivery for drugs targeting the CNS, potentially providing high bioavailability due to avoidance of a hepatic first-pass effect and rapid systemic uptake via perivascular spaces in the respiratory epithelium (Chien, et al., 1989). Apart from that, the olfactory epithelial pathway may allow therapeutic agents to diffuse into the perineural spaces, crossing the cribriform plate, ending up in the cerebral spinal fluid (CSF) (Frey, et al., 1997; Baker and Spencer, 1986). In addition, the olfactory nerve pathway may allow intracellular transport through olfactory sensory neurons, passing the cribriform plate, into the olfactory bulb (Bagger and Bechgaard, 2004). By directly targeting the brain, it has been hypothesized that IN delivery can enhance the CNS target site bioavailability and the efficacy of CNS drugs (Graff and Pollack, 2005; Illum, 2004; Jansson and Bjork, 2002).

Typically, IN administration data are compared to various other administration routes, on the basis of area under the curve (AUC) of plasma-, and CSF concentration-time profiles. However, although CSF-over-plasma AUC ratios reflect differences in exposure after IN administration (Van den Berg, et al., 2004), it does not allow the distinction between direct nose-to-brain transport and systemic uptake in terms of absorption rate and bioavailability. Consequently, the existence of a direct nose-to-brain route is still a

matter of debate (Dhuria, et al., 2009). PK modeling would provide the opportunity to quantify the systemic- and direct nose-to-brain absorption separately, which is not possible on the basis of AUC comparison.

Another important factor is that CSF concentrations do not necessarily reflect target site concentrations (De Lange and Danhof, 2002). This is because of factors related to CSF turnover, intra-brain diffusion, extra-intracellular exchange, and qualitative and quantitative differences in BBB and blood-CSF-barrier transport mechanisms. As many targets (receptors) are facing the brain extracellular fluid (ECF), brain ECF concentrations are anticipated to reflect target site concentrations best, and will therefore provide a better basis to describe pharmacokinetic (PK)- and pharmacodynamic (PD) relations in a more mechanistic manner (Del Bigio, 1994; De Lange, et al., 1999; De Lange and Danhof, 2002; De Lange, et al., 2005; Watson, et al., 2009; Jeffrey and Summerfield, 2010).

Our interest is to investigate the PK-PD mechanisms that play a role in modulation of the dopaminergic system, and the use of IN administration of dopaminergic drugs that often encounter very low bioavailability and/or limited BBB transport. The aim of the study was to quantitatively assess direct transport of remoxipride into the brain following IN administration. Remoxipride is a weak, but selective, dopamine-D2 receptor antagonist (Farde and Von Bahr, 1990; Köhler, et al., 1990; Ogren et al., 1993) and was prescribed as an atypical antipsychotic (Roxiam®) at the end of the eighties. Due to a few cases of aplastic anemia, the drug was withdrawn from the market (Philpott, et al., 1993). However, remoxipride is still of interest as a paradigm compound in mechanism-based PK-PD studies on the dopaminergic system.

Using our previously reported minimum stress, freely moving rat model for IN and IV drug administration (Stevens, et al., 2009), plasma- and brain ECF samples were obtained over time, following IV- and IN administration of 4, 8, or 16 mg/kg remoxipride. Compartmental PK non-linear mixed effects

modeling using NONMEM (Beal and Sheiner, 1992)) was applied to quantify the direct nose-to-brain distribution in terms of absorption rate and bioavailability.

# Methods

## Animals

All animal procedures were performed in accordance with Dutch laws on animal experimentation. The study protocol was approved by the Animal Ethics Committee of Leiden University (UDEC 6132). Male Wistar WU rats (n=60, 253 ± 20 g, Charles River, The Netherlands) were housed in groups for 7-13 days (Animal Facilities, Gorlaeus Laboratoria, Leiden, The Netherlands), under standard environmental conditions (ambient temperature 21°C; humidity 60%; 12/12 hour light, background noise, daily handling), with *ad libitum* access to food (Laboratory chow, Hope Farms, Woerden, The Netherlands) and acidified water. Between surgery and experiments, the rats were kept individually in Makrolon type 3 cages for 7 days to recover from the surgical procedures.

## Surgery

Rat surgery and experiments were performed as previously reported (Stevens, et al., 2009). In short, during anaesthetized surgery, all animals received cannulas in the femoral artery and vein for serial blood sampling and drug administration respectively. Also, an IN probe (AP 12mm and L –0.5 mm relative to Bregma) for drug administration, and a microdialysis guide (caudate putamen; AP +0.4, L 3.2, V -3.5 relative to Bregma), were implanted. After 6 days, the microdialysis guide was replaced by a microdialysis probe (CMA/12, 4 mm Polycarbonate membrane, cut-off 20 kD, Aurora Borealis Control, Schoonebeek, The Netherlands) for continuous brain ECF sampling (Chaurasia, et al., 2007). At 24 ± 1 hour later, the experiments were started.

## Experiments

The rats were randomly assigned to 3 groups (n=20 per group), to receive 4, 8, or 16 mg remoxipride (Tocris, Bristol, United Kingdom) per kg bodyweight. Per group, at time=0 min (corresponding with actual time of 10 AM ± 1 h), remoxipride in saline (B. Braun Melsungen AG, Melsungen, Germany) was administered via either a 1-minute IN infusion (n=10), or a 30-minute IV infusion (n=10), using an automated pump (Harvard apparatus 22, model 55-2222, Holliston, MA, USA). For the IN infusions, different remoxipride solutions were used to ensure similar flow rates (± 19 µl/min) and total IN administered volumes.

Before the experiments, perfusion fluid consisting of 145 mM NaCl, 0.6 mM KCl, 1.0 mM $MgCl_2$ , 1.2 mM $CaCl_2$ , 0.2 mM ascorbic acid, in a 2 mM potassium phosphate buffer, pH 7.4 (Moghaddam and Bunney, 1989) was prepared. From t= -30 to 240 min, the microdialysis probe was continuously flushed with perfusion fluid at a flow rate of 2 µl/min. Microdialysate samples were collected every 10 minutes for the first 2 hours, and every 20 minutes thereafter until the end of the experiments and collected in a cooled fraction collector (Univentor 820 Microsampler, Antec, Netherlands). The microdialysis samples were weighed to confirm accurate sampling volumes and stored at -80˚C, pending analysis. Microdialysis samples were considered accurate and further used only when their volume was within 95-105% of the expected volumes of 20 or 40 µl for 10- and 20 minute samples respectively. Blood samples of 200 µl each were taken from the arterial cannula at time = -5 (blank), 5, 10, 20, 35, 60, 90, 120, 150, 180, and 240 minutes and collected in EDTA-coated vials. After centrifuging for 15 minutes at 5000 rpm, the plasma was stored at -20˚C. After the experiments, the animals were decapitated following an overdose of Nembutal (1 ml, IV).

Two animals from the 4 mg/kg IN dosing group were excluded as the nasal cannula was partially blocked. At some instances during plasma sampling, the arterial cannula was blocked, thereby preventing further sampling. Ultimately, 350 plasma and 235 brain ECF samples could be obtained from 58 remoxipride

DMD Fast Forward. Published on September 8, 2011 as DOI: 10.1124/dmd.111.040782
This article has not been copyedited and formatted. The final version may differ from this version.



treated rats and were analyzed for remoxipride. The IV study consisted of 190 plasma-, and 126 brain ECF data points, the IN study of 160 plasma-, and 109 brain ECF data points.

## Analytical Methods

Analytical methods for the quantitation of remoxipride in small plasma- and brain microdialysate samples have been previously reported (Stevens, et al., 2010). In short, for the measurements of remoxipride concentrations in plasma, online solid phase extraction was followed by high-pressure liquid chromatography-tandem mass spectrometry (Finnigan TSQ Quantum Ultra Mass Spectrometer System, Thermo Fischer Scientific, Breda, The Netherlands). Brain microdialysate samples were measured using high-pressure liquid chromatography-tandem mass spectrometry, without sample clean up. Remoxipride concentrations in microdialysate samples were corrected for *in vivo* recovery through the microdialysis probe and tubing (based on *in vivo* loss (20, 100 and 500 ng/ml), with mean ± S.E.M. = 20 % ± 0.6), to yield estimates of brain ECF concentration values (Chaurasia, et al., 2007). Data acquisition and processing was performed using LC-Quan provided by Thermo Fisher Scientific. For constructing the calibration curve, linear regression analysis was applied using weigh factor $1/Y^2$. The lower limits of detection were 0.15 and 0.08 ng/ml remoxipride in plasma- and in microdialysate samples respectively. The lower limits of quantification were 0.5 and 0.25 ng/ml for plasma and microdialysate samples respectively.

Using the obtained individual plasma- and brain ECF profiles, mean AUC ± S.E.M values were calculated per matrix (plasma /brain ECF), dose (4,8,16 mg/kg) - and study (IN/ IV) group, using the trapezoidal rule (from time = 0 min until the end of experiments).

## Pharmacokinetic model building and random variability

Nonlinear mixed effect modeling using NONMEM (version VI, level 2.0, Icon Development Solutions, Ellicott City, Maryland, USA) was used for the structural model building, performed under ADVAN 6,

and the first order conditional method with interaction was used for estimation with a convergence criterion of 3 significant digits in the parameter estimates. NONMEM reports an objective function value (OFV), which is the -2*log likelihood. Model hypothesis testing was done using the likelihood ratio test under the assumption that the difference in -2*log likelihood is Chi-square distributed with degrees of freedom determined by the number of additional parameters in the more complex model. Hence, with a decrease in the OFV of at least 3.84 points ($p < 0.05$) the model with one additional parameter is preferred over its parent model.

Additive, proportional, or combined residual variability models were investigated separately for the remoxipride concentrations in plasma and in brain ECF(measurement compartments). Log normal distribution of the inter-individual variability (IIV) was assumed and possible covariate correlations were taken into account. Calculation of the coefficient of variation (CV) was used to derive the uncertainty in the parameter estimates of the model, and considered acceptable when lower than 50%. By this approach, several compartmental model structures were optimized (Fig. 1).

Typical values for the PK parameters clearance (CL), volume of distribution (V), and inter-compartmental clearance (Q, clearance between the compartments) were estimated, based on parameter estimates ($\theta$). When identifiable, a term expressing IIV ($\eta$) was included (equation 1).

*Equation 1; Typical value* $= \theta * e^{\eta}$

Transport of remoxipride over time between the compartments and elimination processes were defined by rate constants (equation 2) based on the typical estimated values for CL (or Q) and V.

*Equation 2;* $k_{x,y} = CLxy/Vx$

In model 1, plasma and brain ECF data following IV administration of remoxipride were simultaneously modeled in a structural model consisting of a central, a brain and a peripheral compartment (Fig. 1, model 1). For the elimination of remoxipride from plasma, a first order elimination rate constant was applied

DMD Fast Forward. Published on September 8, 2011 as DOI: 10.1124/dmd.111.040782
This article has not been copyedited and formatted. The final version may differ from this version.



($k_{30}$). As removal of remoxipride from the brain was underestimated, an additional first order elimination rate constant ($k_{40}$) was applied in a second structural model approach (Fig. 1, model 2). The value for $k_{40}$ was assumed to be smaller than $k_{30}$, and therefore calculated as the estimated fraction of $k_{30}$ (equation 3).

*Equation 3;* $k_{40} = (\theta * e^{\eta}) * k_{30}$

As models 1 and 2 are nested (based on identical datasets), their OFVs can be used as comparative means to identify the model that best describes the data, taking into account the number of additional parameters. These two models formed the basis for the identification of more complex model structures that include the IN dataset.

For inclusion of the IN dataset, an absorption compartment with an absorption rate constant (ka) was added to the model structure, here as $ka_{13}$. In the first instance, $ka_{13}$ and bioavailability from the site of absorption to the central plasma compartment ($F_1$) were estimated, leaving out brain elimination (Fig. 1, model 3). An improvement was made by addition of $k_{40}$ (Fig. 1, model 4) using the same approach as for model 2.

In the final model (5), a second absorption compartment was added, describing the hypothesized direct nose-to-brain transport. Absorption from the IN site of administration to the brain results from transport of compound over a longer distance when compared to systemic absorption, as the latter depends on the nasal vascular system that is closely located to the site of administration. As a result, direct nose-to-brain transport is a relatively slow process compared to systemic absorption (Dhuria, et al., 2009). Therefore, typical values for the absorption rate constants were estimated on the assumption that the absorption rate constant to the central compartment ($ka_{13}$) is higher than the absorption rate constant into the brain compartment ($ka_{24}$). The total bioavailability ($F_{TOT}$) was defined as the sum of the bioavailability to the central compartment ($F_1$) and that for the brain compartment ($F_2$). During model optimization, typical values for $F_1$ and $F_{TOT}$ were estimated, whereas $F_2$ was calculated ($F_2=F_{TOT}-F_1$). The change in amount of

DMD Fast Forward. Published on September 8, 2011 as DOI: 10.1124/dmd.111.040782
This article has not been copyedited and formatted. The final version may differ from this version.



remoxipride (dA) in each compartment over time (dt) was described using differential equations (equations 4-8).

*Equation 4; Nose-to-systemic absorption:* $dA_{ABS1}/dt = - A_{ABS1}*ka_{13}$

*Equation 5; Nose-to-brain absorption:* $dA_{ABS2}/dt = - A_{ABS2}*ka_{24}$

*Equation 6; Central absorption and elimination:* $dA_{central}/dt = A_{ABS1}*ka_{13}-A_{central}*k_{34}+A_{brain}*k_{43}-A_{central}*k_{35}+A_{periph}*k_{53}-A_{central}*k_{30}$

*Equation 7; Brain absorption and elimination:* $dA_{brain}/dt = A_{ABS2}*ka_{24} +A_{central}*k_{34}-A_{brain}*k_{43}-A_{brain}*k_{40}$

*Equation 8; Peripheral distribution and elimination:* $dA_{periph}/dt = A_{central}*k_{35}-A_{periph}*k_{53}$

The optimized models 3, 4 and 5 are nested and were therefore compared on the basis of OFV.

## Model evaluation

All optimized models were internally qualified based on goodness-of-fit for individual concentration-time profiles in plasma and brain ECF. As for the intravenous administration groups doubling of the dose leads to doubling of the values for plasma- and brain ECF AUC's, BBB transport of remoxipride was not considered to be subjected to active influx- or efflux processes. Hence, observed remoxipride concentrations were normalized to dose (16 mg/kg) before performance of a visual predictive check (VPC). The VPCs were performed using NONMEM VI, by simulating 1000 replications of the PK model and a simulation dataset that contained dosing information for one individual rat per dosing regimen and administration group. The median, 5 and 95 percentiles were calculated for each simulated time-point. The predictions at each time-point (median and 90 % prediction interval) were compared visually with the actual normalized data. Resemblance between simulated and original distributions indicates the accuracy of the model (i.e., 90 % of the observed data should fall within the predicted range for 90 % of the variability) (Post, et al., 2008).

DMD Fast Forward. Published on September 8, 2011 as DOI: 10.1124/dmd.111.040782
This article has not been copyedited and formatted. The final version may differ from this version.



# Results

## Remoxipride plasma and brain ECF data following IV and IN administration

Plasma concentration-time profiles of remoxipride following IV- and IN administration of 4, 8 and 16 mg/kg of remoxipride are shown in figure 2A. The maximal remoxipride concentration ($C_{max}$) in plasma is higher following IV administration, when compared to the $C_{max}$ following IN administration of a similar dose. Moreover, the slope of the concentration-time profile during the elimination phase seemed to be slower following IN compared to IV administration, and indicates slow absorption processes.

The brain ECF concentration-time profiles are shown in figure 2B. The $C_{max}$ for brain ECF concentrations after IN administration was lower than the $C_{max}$ following IV administration. Furthermore, following IN administration, remoxipride brain ECF concentrations decreased slower when compared to IV administration. As a consequence, the $AUC_{brain\ ECF}/AUC_{plasma}$ ratio value following IN administration was higher when compared to IV administration (Table 1). This indicates direct nose-to-brain transport (Van den Berg, et al., 2004).

Doubling of the dose (4 to 8 to 16 mg/kg) resulted in doubling of the mean $AUC_{plasma}$ and $AUC_{brainECF}$ in both IV and IN studies (Table 1), indicating linear BBB distribution.

## Development of the structural PK model for simultaneous analysis of IN and IV data

The plasma- and brain ECF remoxipride concentrations following IV and IN administration were modeled in NONMEM VI. Several structural models were examined to investigate brain elimination and hypothesized direct nose-to-brain transport (see Methods for details). Table 2 summarizes the OFVs, parameter estimates with their precision (CV), IIV and residual error for all structural models. Because of

DMD Fast Forward. Published on September 8, 2011 as DOI: 10.1124/dmd.111.040782
This article has not been copyedited and formatted. The final version may differ from this version.



linear BBB distribution, all the observed plasma- and brain ECF concentrations could be normalized to dose before performing VPCs.

**IV data**

For data obtained following IV administration of remoxipride, model 1 consisted of a central, peripheral and brain compartment (Fig. 1). Parameter estimates showed low CVs (< 25%), indicating good precision for all typical parameter estimates. A relatively large IIV was identified for CL3 and V5, while a proportional error model best described the residual error in both measurement compartments. The median of the plasma VPC of model 1 (Fig. 3), shows good prediction of the $C_{max}$ in plasma, but the concentrations during elimination were under-predicted. All the brain ECF concentrations were over-predicted by the model. The variability could not be adequately estimated as indicated by large confidence interval of the VPCs, when compared to the original distribution.

Addition of brain elimination in model 2 (Fig.1) showed improved model predictions for plasma and brain ECF observations (Fig. 3). The brain ECF observations were now randomly distributed around the simulated median, indicating improved accuracy of the model. The OFV was improved compared to model 1 (328 points) and IIV was identified for the same parameters. Overall, the CVs were decreased compared to model 1, indicating better estimation of parameter estimates. Based on the overall decrease in values for IIV and residual errors (proportional), model 2 was better able to accurately estimate the variability as well.

**IV and IN data**

Following IN administration, a single systemic absorption compartment (Fig. 1, model 3) allowed for parameter estimation with low CVs. The plasma concentrations of the IV study were well described by VPC median of model 3 (Fig. 3). However, the brain ECF concentrations following IV administration were poorly predicted. Specifically, the $C_{max}$ was over-predicted and, although for the elimination phase the slope of the median followed the slope of the observations, there was over-prediction of the observed concentrations for the full time range. After IN administration, model 3 under-predicted the $C_{max}$ in

DMD Fast Forward. Published on September 8, 2011 as DOI: 10.1124/dmd.111.040782
This article has not been copyedited and formatted. The final version may differ from this version.



plasma and the brain ECF observations were not randomly distributed around the simulated median due to over-prediction of the high concentration range (including $C_{max}$) and under-predicting the lower concentration range. Significant IIV variability was identified on CL3, V4, $ka_{13}$, and $F_1$, and a proportional error model best described residual error in the central- and brain compartment. Since the parameter estimates did not allow good predictions of the brain ECF observations, total bioavailability could not be accurately estimated.

Again, incorporation of brain elimination in the model (model 4) greatly improved the OFV (424 points). Also, the VPC median for the brain ECF concentration-time profiles after IV administration was better when compared to model 3 (Fig. 3), albeit that still a slight under-prediction of $C_{max}$ and over-prediction of concentrations during the elimination phase was observed. Specifically, after IN administration, the $C_{max}$ in brain ECF was under-predicted, as were all concentrations during the elimination phase. The uncertainties for the parameter estimates (CV) were slightly higher, IIV variability was identified on CL3, V4, $ka_{13}$, and $F_1$, and a proportional error model best described residual error in both measurement compartments.

The final model (Fig. 1, model 5) took into account a second, direct transportation route from the nasal cavity to the brain ECF compartment, as well as brain elimination. In contrast to model 4, the VPC (Fig. 4) showed good prediction for both the plasma- and brain ECF concentrations after IV administration. The plasma observations after IN administration were also accurately described. The major advancement of the final model was represented in the median of the brain ECF VPC, which described the observations well, although a minor under-prediction of the $C_{max}$ and elimination phase was observed. This led to a highly significant improvement in goodness-of-fit compared to model 4 (OFV decrease from -3239 to -3435). The majority of the observations for IN- and IV administration were within the 90% prediction interval. The CVs decreased for all estimated parameters, indicating improved certainty for the parameter estimations. In addition to the IIV on CL3, V4, $ka_{13}$, and $F_1$ in the previous model, IIV could also be

identified for V5 and $F_{TOT}$. Again, proportional error models best described the residual error in both plasma and brain ECF compartments.

Since the remoxipride concentrations were accurately predicted in both plasma- and brain ECF, the absorption rate constant- and bioavailability parameter estimates can be considered accurate. In the final model, the low value of the absorption rate constant to the brain ($ka_{24}$) represents slow transport mechanisms from the nose to the brain and showed a relatively high CV (43.8%). The bioavailability of direct nose-to-brain transport was found to be 75% ($F_2/F_{TOT}$) of the $F_{TOT}$ (89%). The $ka_{24}$ was low when compared to the $ka_{13}$, explaining the relative slow decrease in plasma- and brain ECF concentrations over time following IN administration. This indicates fast absorption into plasma and consecutive BBB transport, after which concentrations in brain ECF are maintained by (slower) direct nose-to-brain transport. IIV for $F_{TOT}$ was found to be 0.48. Furthermore, the use of dense, serial blood and microdialysis sampling allowed for a precise estimation of the $F_{TOT}$ (CV of only 4.6%).

Further data analysis showed a smaller apparent total volume of distribution when comparing models 2 and 5. These factors indicate a more complex distribution from the nasal cavity to the site of measurement. Addition of absorption and/or brain compartments were considered in the early phase of the structural model building, e.g. dual (slow and fast) direct nose-to-brain transport or an extra compartment between the absorption- and brain compartment. However, additional absorption processes and/or compartments could not be identified with the present dataset from our animal model.

## Discussion

The aim of the study was to quantitatively assess direct transport of remoxipride into the brain following IN administration. To this end, plasma- and brain ECF concentration-time profiles were obtained following IV and IN administration of 3 different dosages, and data were analyzed using a PK modeling approach. A multi-compartment, semi-physiologically-based PK model with one absorption compartment from the nose into the systemic circulation and one from the nose into the brain compartment was found to best describe the observed data. Total bioavailability following IN administration was 0.89, of which 75% was attributed to direct nose-to brain transport. The absorption rate constant from the nose to the brain was low when compared to the absorption rate constant for systemic uptake, explaining the relatively slow decrease in plasma- and brain ECF concentrations over time following IN administration. These studies explicitly provide separation and quantitation of systemic- and direct nose-to-brain transport after IN administration.

To characterize BBB transport in rats, increasing and decreasing remoxipride concentrations in plasma- and brain ECF over time were obtained using 30-minute IV infusion. For IN administration, the duration of the intranasal administration was restricted by maximum solubility of remoxipride and the maximum administration volume in freely moving rats (Stevens, et al., 2009). At later time points (> 150 min), the mean concentration-time profiles of remoxipride in brain ECF after intravenous administration of the 4 mg/kg dose group is higher than the 8 and 16 mg/kg dose groups (Fig. 2B). Using a small number of animals in each group, effects of interindividual variability can explain the inconsistency for this single dose group, as is taken into account by population-based modeling. Although highly unlikely, we cannot fully exclude a potential structural difference in brain ECF exposure between the 4 mg/kg and higher dose regimens. Also considering the fact that plotting on a semi logarithmic scale puts higher visual emphasis on the lower concentrations range, we did not include potential structural differences for the lowest dose group in our modeling approach.

DMD Fast Forward. Published on September 8, 2011 as DOI: 10.1124/dmd.111.040782
This article has not been copyedited and formatted. The final version may differ from this version.



Standard nonparametric analysis of our data showed that BBB transport was linear. Although no preclinical literature could be found to compare these results, in schizophrenic patients remoxipride readily passes the BBB (Farde and Von Bahr, 1990). Furthermore, as only free drug concentrations can cross the BBB, protein binding needs to be considered. Slight concentration dependent plasma binding has been reported in patients with tardive dyskinesia (Widerlov, et al., 1991), however, we did not find any indication for this in our dose range. As BBB transport appeared to be linear and measurements were taken in the plasma- and brain compartment, Q4 represents movement of unbound remoxipride concentrations, thereby incorporating protein binding.

Despite an approximate doubling of $C_{max}$ in plasma and brain ECF for IV compared with IN administration, the elimination is slower for the latter (Fig. 2). The slower elimination for IN indicates an absorption rate dependent elimination rate (flip-flop kinetics), being most pronounced in the brain ECF (Fig. 3). The resulting increase of $AUC_{brain\ ECF}/AUC_{plasma}$ for IN when compared to IV administration (Table 1), suggests direct nose-to-brain transport (Van den Berg, et al., 2004). For remoxipride it seems that a fast onset of action can be reached by the fast systemic uptake, while the slower direct nose-to-brain transport is expected to result in a prolonged duration of effect after intranasal administration.

In model 1, the VPCs revealed misspecification of the brain ECF concentration predictions. Hepatic clearance and urinary excretion are known to result in elimination of remoxipride from plasma (Widerlov, et al., 1989;Widman et al., 1993;Nilsson, 1998), as was included in our model approaches by the first order elimination rate constant $k_{30}$. An additional parameter for brain-elimination was essential to predict both plasma- and brain ECF observations adequately (model 2), indicating that more complex processes are responsible for the clearance of remoxipride from the brain ECF. The main metabolic routes in rodents are 1) hydroxylation and 2) *O*-demethylation at the aromatic moiety of remoxipride. Remoxipride metabolites have been previously identified in rat brain, and have been contributed to liver metabolism and consecutive BBB transport (Ahlenius, et al., 1997). However, in another study, *O*-demethylase activity has been identified in rat brain (Jolivalt, et al., 1995), which could account for brain metabolism

DMD Fast Forward. Published on September 8, 2011 as DOI: 10.1124/dmd.111.040782
This article has not been copyedited and formatted. The final version may differ from this version.



of remoxipride. To our knowledge, there are no studies that implicate remoxipride as a substrate for brain efflux transporters. In our model, the clearance processes in the brain were lumped in a single first order elimination rate constant ($k_{40}$), awaiting more mechanistic data on brain elimination processes (e.g. by *in vitro* studies) to further develop the model for specific mechanistic understanding.

Simultaneous analysis of the IV and IN datasets using models 3 and 4 yielded the consistent finding that brain elimination is essential to predict brain ECF remoxipride concentrations. However, this approach could not explain the slower decrease in remoxipride concentrations in brain ECF following IN administration. The final model took into account a second, direct transportation route from the nasal cavity to the brain ECF compartment, as well as brain elimination. This led to a highly significant improvement in goodness-of fit for remoxipride plasma- and brain ECF concentration-time profiles as reflected in the reduction of the OFV, CVs, IIV and improved VPC. Consequently, the bioavailability parameters could be considered precise.

Regarding intra-individual variability following IN administration, one has to take into account that there are many protective barriers in the nasal cavity, such as mucocilliary clearance, efflux transporter proteins and metabolizing enzymes that influence the absorption of compounds (Dhuria, et al., 2009), which may all contribute. The low value found for the $ka_{24}$ (0.033 /h) represents slow transport mechanisms via the olfactory epithelial- and/or olfactory nerve pathway, that are both subject to IIV. Although IIV on $ka_{24}$ as such could not be identified, it may explain the lower precision of $ka_{24}$, when compared to $ka_{13}$, the latter which is associated with a smaller absorption distance. It would be of interest to quantify the olfactory epithelial- and nerve pathways separately, which is not possible with the current dataset. In future investigations, measuring remoxipride brain ECF concentrations simultaneously in several brain regions could allow the quantification of separate absorption rate constants for the different direct nose-to-brain transport routes.

From our studies, it is clear that brain ECF concentrations are influenced by direct nose-to-brain transport, BBB transport following systemic uptake and brain elimination processes. To understand the effect of CNS-active drugs, it is pertinent to understand the drug exposure at the target site (brain ECF) as this provides a better basis for the determination of concentration-effect relationships following IN administration. In humans, information on target site distribution is more difficult to obtain when compared to animal studies. However, based on preclinically derived semi-physiologically-based PK parameters, translational modeling would allow simulation of human brain ECF concentrations, which can form the basis of PK-PD models that will help towards increased safety and efficacy (Danhof, et al., 2008). Small scale, efficient clinical trials could subsequently provide the accuracy of these preclinical derived translational models.

In conclusion, by simultaneous modeling of plasma- and brain ECF concentrations-time profiles obtained following IV and IN routes of administration of remoxipride, we have provided a semi-physiologically-based PK model on the target site distribution of remoxipride. The model provides quantitative evidence of direct nose-to-brain transport after IN administration. Also, pharmacokinetic modeling allowed the quantification of brain elimination, which contributed significantly to clearance of remoxipride. Further investigations on the plasma- and brain ECF PK of other compounds should lead to a more generalized model for IN administration, since direct nose-to-brain transport is compound dependent. Describing rat brain PK in a semi-physiology based manner is anticipated to allow for simulation of human brain ECF concentrations by means of translational models. This will aid in the prediction of the efficacy and safety of CNS active compounds after IN administration in man.

## Authorship Contributions

*Participated in research design*: Stevens, Van der Graaf, Danhof, De Lange

*Conducted experiments*: Stevens

*Contributed new reagents or analytic tools*: Ploeger

*Performed data analysis*: Stevens, Ploeger

*Wrote or contributed to writing of the manuscript*: Stevens, Ploeger, Van der Graaf, Danhof, De Lange

## References

Ahlenius S, Ericson E, Hillegaart V, Nilsson LB, Salmi P and Wijkstrom A (1997) In Vivo Effects of Remoxipride and Aromatic Ring Metabolites in the Rat. *J Pharmacol Exp Ther* **283**:1356-1366.

Bagger MA and Bechgaard E (2004) The potential of nasal application for delivery to the central brain-a microdialysis study of fluorescein in rats. *Eur J Pharm Sci* **21**:235-242.

Baker H and Spencer RF (1986) Transneuronal transport of peroxidase-conjugated wheat germ agglutinin (WGA-HRP) from the olfactory epithelium to the brain of the adult rat. *Exp Brain Res* **63**:461-473.

Beal SL and Sheiner BL (1992) *NONMEM user's guide, Part 1*, University of California at San Francisco, San Francisco.

Chaurasia CS, Muller M, Bashaw ED, Benfeldt E, Bolinder J, Bullock R, Bungay PM, DeLange ECM, Derendorf H, Elmquist WF, Hammarlund-Udenaes M, Joukhadar C, Kellogg DL, Jr., Lunte CE, Nordstrom CH, Rollema H, Sawchuk RJ, Cheung BWY, Shah VP, Stahle L, Ungerstedt U, Welty DF and Yeo H (2007) AAPS-FDA Workshop White Paper: Microdialysis Principles, Application, and Regulatory Perspectives. *J Clin Pharmacol* **47**:589-603.

Chien WY, Su KSE and Chang SF (1989) *Nasal systemic drug delivery*, Marcel Dekker Inc., New York.

Danhof M, De Lange EC, Della Pasqua OE, Ploeger BA and Voskuyl RA (2008) Mechanism-based pharmacokinetic-pharmacodynamic (PK-PD) modeling in translational drug research. *Trends Pharmacol Sci* **29**:186-191.

De Lange EC, Bouw MR, Mandema JW, Danhof M, De Boer AG and Breimer DD (1995) Application of intracerebral microdialysis to study regional distribution kinetics of drugs in rat brain. *Br J Pharmacol* **116**:2538-2544.

De Lange EC and Danhof M (2002) Considerations in the use of cerebrospinal fluid pharmacokinetics to predict brain target concentrations in the clinical setting: implications of the barriers between blood and brain. *Clin Pharmacokinet* **41**:691-703.

De Lange EC, De Boer BA and Breimer DD (1999) Microdialysis for pharmacokinetic analysis of drug transport to the brain. *Adv Drug Deliv Rev* **36**:211-227.

De Lange EC, Ravenstijn PG, Groenendaal D and Van Steeg TJ (2005) Toward the prediction of CNS drug-effect profiles in physiological and pathological conditions using microdialysis and mechanism-based pharmacokinetic-pharmacodynamic modeling. *AAPS J* **7**:E532-E543.

Del Bigio MR (1994) The ependyma: A protective barrier between brain and cerebrospinal fluid. *Glia* **14**:1-13.

Dhuria SV, Hanson LR and Frey WH (2009) Intranasal delivery to the central nervous system: Mechanisms and experimental considerations. *Journal of pharmaceutical sciences* **99**:1654-1673.

Farde L and Von Bahr C (1990) Distribution of remoxipride to the human brain and central D2-dopamine receptor binding examined in vivo by PET. *Acta Psychiatr Scand Suppl* **358**:67-71.

Frey WH, Liu J, Chen X, Thorne RG, Fawcett JR, Ala TA and Rahman Y (1997) Delivery of 125-I-NGF to the brain via the olfactory route. *Drug delivery* **4**:87-92.

Graff CL and Pollack GM (2005) Nasal drug administration: potential for targeted central nervous system delivery. *J Pharm Sci* **94**:1187-1195.

Illum L (2004) Is nose-to-brain transport of drugs in man a reality? *J Pharm Pharmacol* **56**:3-17.

Jansson B and Bjork E (2002) Visualization of in vivo olfactory uptake and transfer using fluorescein dextran. *J Drug Target* **10**:379-386.

Jeffrey P and Summerfield S (2010) Assessment of the blood-brain barrier in CNS drug discovery. *Neurobiol Dis* **37**:33-37.

Jolivalt C, Minn A, Vincent-Viry M, Galteau MM and Siest G (1995) Dextromethorphan O-demethylase activity in rat brain microsomes. *Neuroscience Letters* **187**:65-68.

Köhler C, Hall H, Magnusson O, Lewander T and Gustafsson K (1990) Biochemical pharmacology of the atypical neuroleptic remoxipride. *Acta Psychiatr Scand Suppl* **358**:27-36.

Moghaddam B and Bunney BS (1989) Ionic composition of microdialysis perfusing solution alters the pharmacological responsiveness and basal outflow of striatal dopamine. *J Neurochem* **53**:652-654.

Nilsson LB (1998) High sensitivity determination of the remoxipride hydroquinone metabolite NCQ-344 in plasma by coupled column reversed-phase liquid chromatography and electrochemical detection. *Biomed Chromatogr* **12**:65-68.

Ogren SO, Lundstrom J, Nilsson LB and Widman M (1993) Dopamine D2 blocking activity and plasma concentrations of remoxipride and its main metabolites in the rat. *J Neural Transm Gen Sect* **93**:187-203.

Philpott N, Marsh JCW, Gordon-Smith EC, Bolton JS, Laidlaw ST, Snowden JA and Brown MJ (1993) Aplastic anaemia and remoxipride. *The Lancet* **342**:1244-1245.

Post TM, Freijer JI, Ploeger BA and Danhof M (2008) Extensions to the visual predictive check to facilitate model performance evaluation. *J Pharmacokinet Pharmacodyn* **35**:185-202.

Stevens J, Suidgeest E, Van der Graaf PH, Danhof M and De Lange EC (2009) A new minimal-stress freely-moving rat model for preclinical studies on intranasal administration of CNS drugs. *Pharm Res* **26**:1911-1917.

Stevens J, Van den Berg D-J, De Ridder S, Niederlander HAG, Van der Graaf PH, Danhof M and De Lange ECM (2010) Online solid phase extraction with liquid chromatography-tandem mass spectrometry

to analyze remoxipride in small plasma-, brain homogenate-, and brain microdialysate samples. *Journal of Chromatography B* **878**:969-975.

Van den Berg MP, Verhoef JC, Romeijn SG and Merkus FW (2004) Uptake of estradiol or progesterone into the CSF following intranasal and intravenous delivery in rats. *Eur J Pharm Biopharm* **58**:131-135.

Watson J, Wright S, Lucas A, Clarke KL, Viggers J, Cheetham S, Jeffrey P, Porter R and Read KD (2009) Receptor occupancy and brain free fraction. *Drug Metab Dispos* **37**:753-760.

Widerlov E, Andersson U, Von Bahr C and Nilsson MI (1991) Pharmacokinetics and effects on prolactin of remoxipride in patients with tardive dyskinesia. *Psychopharmacology (Berl)* **103**:46-49.

Widerlov E, Termander B and Nilsson I (1989) Effect of urinary pH on the plasma and urinary kinetics of remoxipride in man. *European Journal of Clinical Pharmacology* **V37**:359-363.

Widman M, Nilsson LB, Bryske B and Lundstrom J (1993) Disposition of remoxipride in different species. Species differences in metabolism. *Arzneimittelforschung* **43**:287-297.

## Footnotes

a) Pfizer Global Research and Development, Sandwich, England, United Kingdom financially supported this work.

b) Parts of this work were previously presented as follows; Distribution enhancement to the brain after intranasal versus intravenous administration of remoxipride, 6th International Symposium on Measurement and Kinetics of *in vivo* Drug Effects, 2010, April 21-24; Noordwijkerhout, The Netherlands.

# Legends for Figures

*Figure 1; Compartmental model structures. The models consists of 1) an absorption compartment (ABS 1), 2) a second absorption compartment (ABS 2) describing direct nose-to-brain transport, 3) a central measurement compartment (Central; plasma concentrations), 4) a brain measurement compartment (Brain; brain ECF concentrations), and 5) a peripheral compartment (Peripheral) describing the distribution into other tissues and organs. ka, absorption rate constant; k30/k40, first order elimination rate constants; k, rate constants with compartment-associated numbers.*

*Figure 2; Mean concentration-time profiles (± S.E.M.) of remoxipride in plasma (2A) and brain ECF (2B), after 30-minute IV (open symbols), or 1-minute IN (closed symbols) infusion of 4, 8, or 16 mg/kg remoxipride (triangles, circles, and diamonds respectively).*

*Figure 3; The observed remoxipride concentrations (open circles) per study and measurement compartment. The medians of the VPCs of model 1 until 4 are represented by the dotted, dash-dotted, dashed and solid lines respectively.*

*Figure 4; Visual predictive check of the final model, representing the observed remoxipride concentrations (open circles) per study and measurement compartment, the median concentration predictions of the model (black line), and the 90% prediction intervals (grey area).*

DMD Fast Forward. Published on September 8, 2011 as DOI: 10.1124/dmd.111.040782
This article has not been copyedited and formatted. The final version may differ from this version.



# Tables

**Table 1. Mean area's under the curve (± S.E.M.) from 0 to 4 hours of individual plasma- and brain ECFconcentration-time** profiles per study and matrix

| | Intravenous study | | | Intranasal study | | |
|---|---|---|---|---|---|---|
| Dose (mg/kg) | Plasma AUC (μg*min/ml) | Brain ECF AUC (μg *min/ml) | Brain ECF AUC/ plasma AUC (%) | Plasma AUC (μg *min/ml) | Brain ECF AUC (μg *min/ml) | Brain ECF AUC/ plasma AUC (%) |
| 4 | 44.9 (7.7) | 7.9 (1.7) | 17.5 | 10.8 (2.9) | - | - |
| 8 | 70.1 (4.7) | 14.0 (0.7) | 19.9 | 20.0 (5.5) | 4.9 (0.8) | 24.7 |
| 16 | 173.0 (9.0) | 34.6 (7.1) | 20.0 | 53.9 (11.4) | 16.7 (2.4) | 31.0 |
| Mean brain/plasma AUC per study | | | 19 (0.8) | | | 28 (2.6) |

-, not determined

DMD Fast Forward. Published on September 8, 2011 as DOI: 10.1124/dmd.111.040782
This article has not been copyedited and formatted. The final version may differ from this version.

Table 2. Model summary, parameter estimates with coefficients of variation, and calculated pharmacokinetic parameters

| Model summary | Model 1 | Model 2 | Model 3 | Model 4 | Model 5 |
|---|---|---|---|---|---|
| Dataset | IV | IV | IV & IN | IV & IN | IV & IN |
| Brain elimination | No | Yes | No | Yes | Yes |
| Absorption | No | No | 1 | 1 | 2 |
| OFV | -1430 | -1758 | -2815 | -3239 | -3435 |

| Parameter estimate* | TE (CV%) | IIV | TE (CV%) | IIV | TE (CV%) | IIV | TE (CV%) | IIV | TE (CV%) | IIV |
|---|---|---|---|---|---|---|---|---|---|---|
| CL3 (l/h/kg) | 2.22 (12.1) | 0.41 | 0.59 (24.1) | 0.32 | 1.80 (15.2) | 0.38 | 0.36 (36.2) | 0.27 | 1.12 (10.1) | 0.04 |
| V3 (l/kg) | 0.050 (24.2) | ne | 0.062 (16.6) | ne | 0.073 (25.2) | ne | 0.08 (14.8) | ne | 0.088 (13.6) | ne |
| Q4 (l/h/kg) | 0.98 (9.8) | ne | 1.38 (13.3) | ne | 1.66 (27.3) | ne | 1.59 (20.1) | ne | 0.70 (19.9) | ne |
| V4 (l/kg) | 0.41 (39.3) | ne | 1.47 (12.0) | ne | 0.18 (20.7) | 0.31 | 3.02 (40.7) | 0.21 | 0.873 (24.1) | 0.06 |
| Q5 (l/h/kg) | 1.13 (21.6) | ne | 1.18 (11.1) | ne | 0.567 (12.3) | ne | 1.04 (15.6) | ne | 1.20 (10.2) | ne |
| V5 (l/kg) | 0.13 (22.4) | 0.10 | 0.425 (7.9) | 0.05 | 0.325 (7.14) | ne | 0.36 (16.5) | ne | 0.417 (8.60) | 0.08 |
| FK40 (/h) | - | - | - | - | - | - | 0.36 *** | - | 0.302 (17.5) | ne |
| $ka_{13}$ (/h) | - | - | - | - | 1.56 (19.1) | 0.44 | 1.94 (20.7) | 0.35 | 1.54 (11.8) | 0.17 |
| $ka_{24}$ (/h) | - | - | - | - | - | - | - | - | 0.033 (43.8) | ne |
| $F_{TOT}$ | - | - | - | - | - | - | - | - | 0.89 (4.60) | 0.48 |
| $F_1$ | - | - | - | - | 0.171 (22.6) | 0.17 | 0.19 (19.8) | 0.52 | 0.22 (20.1) | 0.09 |
| RV plasma | 0.0629 | | 0.057 | | 0.12 | | 0.11 | | 0.098 | |
| RV microdialysate | 0.48 | | 0.203 | | 0.368 | | 0.19 | | 0.103 | |
| Calculated parameters | | | | | | | | | | |
| $F_2$ | - | | - | | - | | - | | 0.67 | |
| $K_{30}$ (/h) | 44.4 | | 9.5 | | 24.7 | | 4.5 | | 12.7 | |
| $K_{40}$ (/h) | - | | 3.45 (8.9)** | | - | | 1.62 | | 3.84 | |

** parameter estimates are given with their compartment number, according to figure 1; ** estimated parameter; *** fixed parameter;*

*RV, intra individual variability; FK40, k40 as fraction of k30; ne, not estimated in model*

# Figure 1

Model 1

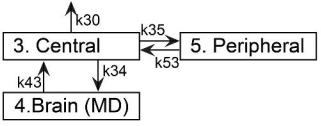


Model 2

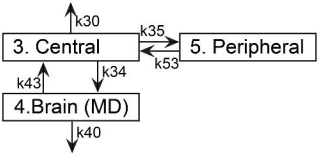


Model 3

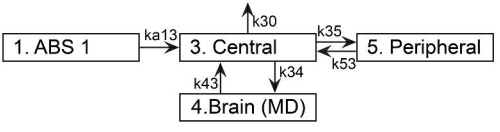


Model 4

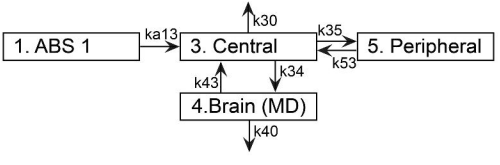


Model 5

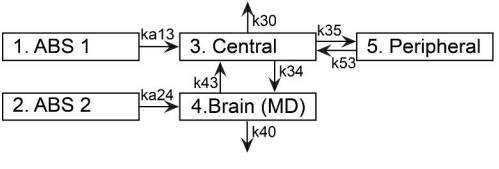

DMD Fast Forward. Published on September 8, 2011 as DOI: 10.1124/dmd.111.040782
This article has not been copyedited and formatted. The final version may differ from this version.

# Figure 2

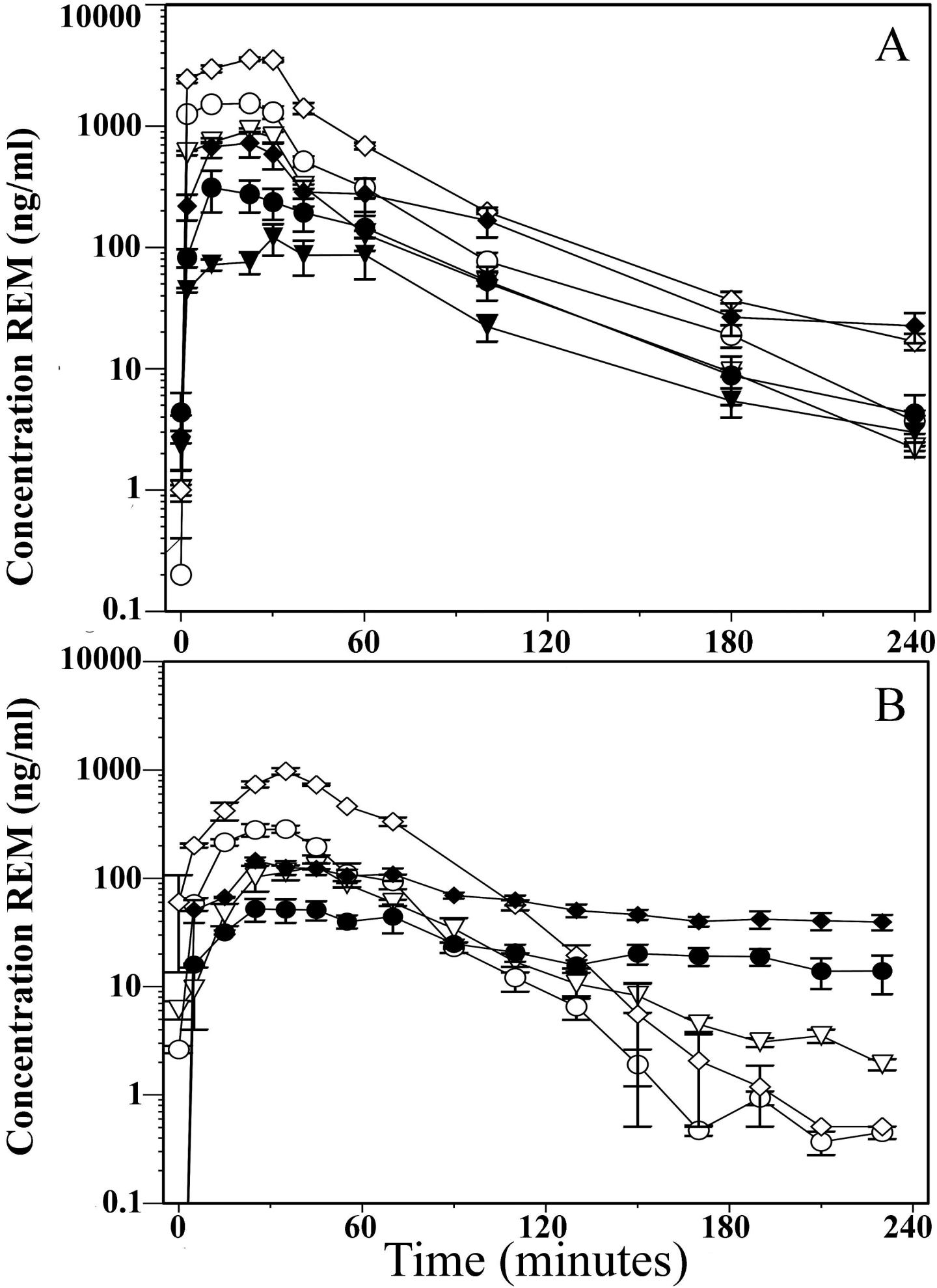

DMD Fast Forward. Published on September 8, 2011 as DOI: 10.1124/dmd.111.040782


# Figure 3

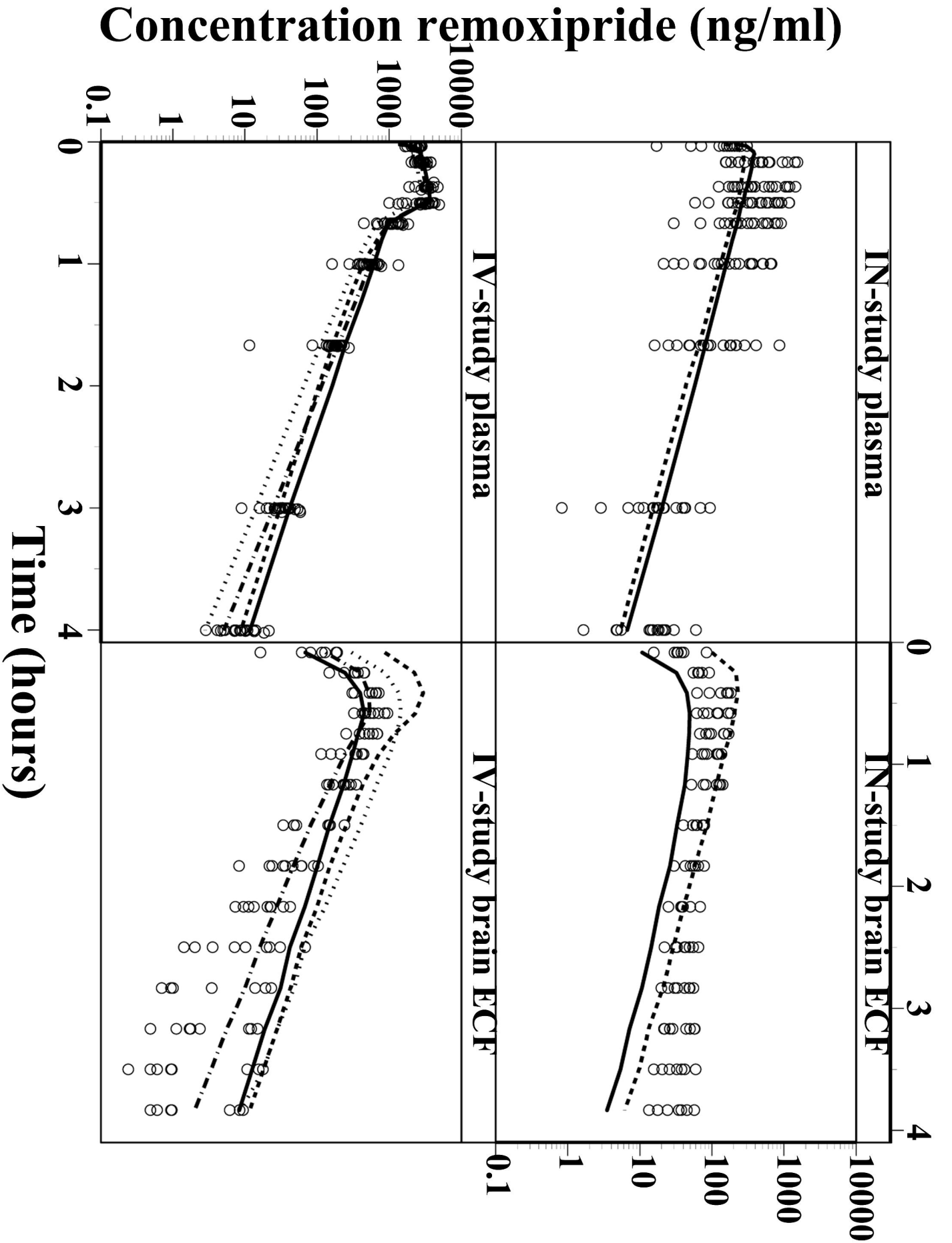

DMD Fast Forward. Published on September 8, 2011 as DOI: 10.1124/dmd.111.040782
This article has not been copyedited and formatted. The final version may differ from this version.

# Figure 4